

Effect of Maleated EVA on Compatibility and Toughness of PETG/EVA Blend

Hae Youn Park,¹ Sung Wook Hwang,² Hee Chang Ryu,³ Sang Woo Kim,⁴ Kwan Ho Seo¹

¹Department of Polymer Science & Engineering, Kyungpook National University, Daegu, Korea

²Korea Packaging Center, Korea Institute of Industrial Technology, Bucheon, Korea

³LG Chem Research Park, LG Chem, Daejeon, Korea

⁴Korean Intellectual Property Office, Daejeon, Korea

Correspondence to: K. H. Seo (E-mail: khseo@knu.ac.kr)

ABSTRACT: Maleic anhydride (MAH) grafted onto ethylene vinyl acetate copolymer (EVA), mEVA (modified EVA) was blended with poly(ethylene glycol-*co*-cyclohexane-1,4-dimethanol terephthalate) (PETG) with various mEVA and EVA (unmodified) content in the internal mixer. The effect of reactive compatibilizer to decrease the dispersed particle diameter was observed. The brittle–ductile transition was found at about d_c : 0.37 μm and d_c : 0.55 μm of particle diameter, a critical particle diameter, regardless of EVA content, and the blend was also toughened at above the critical particle diameter regardless of dispersed EVA content and compatibility. The toughening mechanism and the effect of the particle diameter on the impact strength of the blend were investigated by morphological observation, and it was found that the toughening of the PETG/EVA blend system resulted from the shear deformation, induced by cavitation of dispersed EVA particles. © 2012 Wiley Periodicals, Inc. *J. Appl. Polym. Sci.* 000: 000–000, 2012

KEYWORDS: PETG; EVA; MAH; blends; brittle–ductile transition; toughness

Received 28 June 2011; accepted 23 April 2012; published online

DOI: 10.1002/app.37950

INTRODUCTION

Toughness is an important factor for choosing the polymeric materials where it would be needed, and it is normally accomplished by incorporating the rubbery material into a brittle polymer matrix to make a ductile polymer. This rubber-toughened plastic has been widely investigated by many researchers.^{1,2} There are two types of toughening mechanism by incorporation of rubber particle. High impact polystyrene (HIPS) is the case that rubber particle was well dispersed in polystyrene (PS) matrix, and a multiple crazing is considered as a key toughening mechanism.^{2,3} On the other hand, rubber-toughened nylon,^{2,4,5} rubber-toughened epoxy,^{2,6–8} and rubber-toughened poly(methyl methacrylate; PMMA)^{2,9} are the example of toughening mechanism based on the shear deformation. In this case, the cavitation occurs when the stress is concentrated around rubber particles dispersed in polymer matrix, and shear yielding induces shear deformation resulting in toughening.^{2,10}

Generally, the brittle–ductile transition of polymers with dispersed rubber particle are affected by various parameters such as temperature, rubber particle size, inter-particle distance, and rubber content.^{2,10–14} In addition, it is widely known that

rubber property, the shape of dispersed particle, and interfacial adhesion are the factors that have an effect on polymer toughness.² The rubber particle size and inter-particle distance would be considered as the index to observe how the rubber particle is dispersed in the polymer matrix, and this dispersity are considerably affected by the compatibility of polymers and processing conditions.^{1,15–18} Wu reported that critical distance between particles is an important factor to determine brittle–ductile transition based on his research. He found that the fracture behavior occurred when particle distance was greater than critical value, and polymer could be toughened with the smaller particle distance than critical value.^{2,4,5,19,20} The critical inter-particle distance (τ_c) can be expressed as eq. (1).

$$\tau_c = d_c \left[(\pi/6\Phi_d)^{1/3} - 1 \right] \quad (1)$$

where d_c is the critical dispersed particle diameter, Φ_d is the volume fraction of the dispersed phase

As shown above, the critical inter-particle distance can be obtained from the rubber content and dispersed particle size, so

it could be seen that the smaller particle size in the matrix gives better toughening of the polymers. However, Dompas and Schwier reported that the particle size below 100 nm had a difficulty to have a cavitation, and suggested that there would be a minimum particle size for successful toughening from poly(vinyl chloride) (PVC)/methyl methacrylate-butadiene-styrene graft copolymer (MBS) blends.^{20–22} Bucknall and Andrea reported that deformation begins with cavitation of the rubber particles, and progresses through the growth of dilatational bands from a model for dilatational yielding in rubber-toughened polymers. They suggested that there would not be a cavitation progress when the particle size is too small. In case of rubber-toughened Nylon, the particle size was found to be 0.2 μm to not have a cavitation.²³

In our previous study, it was confirmed that the maleic anhydride (MAH) was grafted onto ethylene vinyl acetate (EVA) under a radical initiator, dicumyl peroxide (DCP), and MAH-g-EVA improved the compatibility of poly(ethylene glycol-co-cyclohexane-1,4-dimethanol terephthalate) (PETG)/MAH-g-EVA blends.²⁴ In this study, PETG, a pseudo-ductile polymer, was used as a matrix, and EVA and MAH-g-EVA were used as dispersion phase. The PETG/EVA/MAH-g-EVA blends with various compositions were prepared, and their impact strength was determined. The effect of morphological changes such as particle content, inter-particle distance, and particle size on the impact strength was investigated, and the toughening mechanism of PETG blends was assessed.

EXPERIMENTAL

Materials

Poly(ethylene glycol-co-cyclohexane-1,4-dimethanol terephthalate; PETG, S2008) as a matrix was provided by the SK Chemicals Ltd. (Seoul, South Korea). PETG is amorphous polymer with 80°C of the glass transition temperature (T_g) and the density was 1.27 g/cm³. Ethylene vinyl acetate copolymer (EVA, VS410) containing 26 wt % of vinyl acetate (VA) with –65 and 73°C of T_g and melting temperature (T_m) was provided by Hyundai Petrochemical Co. (Seoul, South Korea). Melt flow index (MFI) and density were 4.0 g/10 min (ASTM D1238) and 0.950 g/cm³, respectively. Dicumyl peroxide (DCP, 98%) as a radical initiator was purchased from the Aldrich Chemical Co. (St. Louis, MO). Maleic anhydride (MAH) for the graft modification was obtained from Shinyo Pure Chemical Co. (Osaka, Japan) and was used as received.

Preparation of PETG/MAH-g-EVA Blend and the Specimen for Impact Strength

The modification of EVA with MAH was prepared with a Brabender plasti-coder[®] (PLE331; Duisburg, Germany). EVA and 2.0 phr of MAH were initially mixed for 5 min at 175°C, and then 0.1 phr of DCP was added and continued mixing for 10 min. The effect of EVA-g-MAH as a compatibilizer was confirmed at our previous study.²⁴ The Prepared MAH-g-EVA polymer was named with mEVA that is modified and differentiated from uEVA, unmodified EVA. The PETG were blended with mEVA and nEVA with various compositions at a Brabender plasti-coder[®] with a rotor speed of 50 rpm at 210°C for 10 min. The BAU tech mini molder (Bau Tech. BAU-915) was used

to obtain 0.25 mm notched Izod specimen (3 mm \times 75 mm \times 13 mm). The blended sample was mixed at 210°C, and injected into the mold at 190°C, and then annealed at room temperature.

Impact Strength Test and Morphological Observation

The notched Izod impact strength was measured with the Izod impact tester (Testing Machine, TMI 52004) (Ronkonkoma, NY) at room temperature according to ASTM D-256. The morphology of the fractured surface of specimens after the test was investigated by using the field emission scanning electron microscope (FE-SEM, Hitachi S-4300; Japan). The specimens that were not broken through the impact test were also fractured after freezing in liquid nitrogen. The fracture surface was sputter coated with gold and observed. In addition, the image analyzer was also used to determine the particle diameter of dispersed phase. The number average diameter, \bar{d}_n , and volume average diameter, \bar{d}_v , was calculated from the following equations^{25,26}:

$$\begin{aligned}\bar{d}_n &= \frac{\sum n_i d_i}{\sum n_i} \\ \bar{d}_v &= \frac{\sum n_i d_i^3}{\sum n_i d_i^3}\end{aligned}\quad (2)$$

where n_i is the number of particles having the true particle diameter d_i .

RESULTS AND DISCUSSION

Blend Morphology

Figure 1 shows the fractured surface morphology of tested sample of the (a) PETG/uEVA (20 phr) and (b) PETG/mEVA (20 phr). The particle diameter of (b) significantly reduces as compare to (a), and this could be attributed to the improvement of an interfacial adhesion between two components, by decreasing an interfacial tension due to an introduction of the reactive compatibilizer.²⁴ The effect of uEVA and mEVA contents on the particle diameter of the blends was given in Figure 2. It was found that the particle diameter increases as dispersed EVA contents increase, and the blend with mEVA showed smaller particle diameter than uEVA. It also can be seen that the effect of the reactive compatibilizer to reduce the particle diameter was more significant at higher EVA content.

The PETG/(uEVA + mEVA) blends was prepared to observe the effect of mEVA content on the particle diameter of dispersed phase in blends with changing the composition of uEVA and mEVA whereas total EVA content on the blend was fixed at 20 phr. As shown in Figure 3, adding more mEVA in the blends decreases the particle diameter and finally levels off showing that the mEVA has great effect on reducing particle diameter on the blends.

Izod Impact Strength

The impact strength with respect to the EVA content was shown in Figure 4. It was found that the impact strength increases with increasing EVA content and considerably improves at a specific blend composition with the brittle–ductile transition. Interestingly, the transition phenomenon of PETG/mEVA blend occurs at higher EVA content than PETG/uEVA blend. For

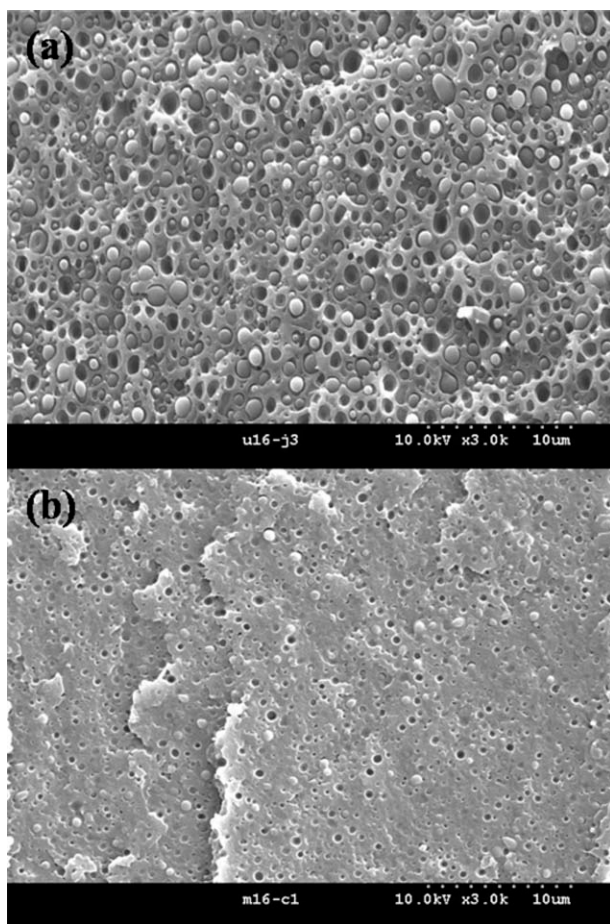


Figure 1. SEM photographs of impact-fractured surface (a) PETG/uEVA (20 phr) and (b) PETG/mEVA (20 phr).

instance, at about 16.7% EVA content, the PETG/mEVA blend having better compatibility than the PETG/uEVA one showed the brittleness whereas the PETG/uEVA presented the ductility.

To investigate the effect of mEVA content on the impact strength in detail, the PETG/(uEVA + mEVA) blends was

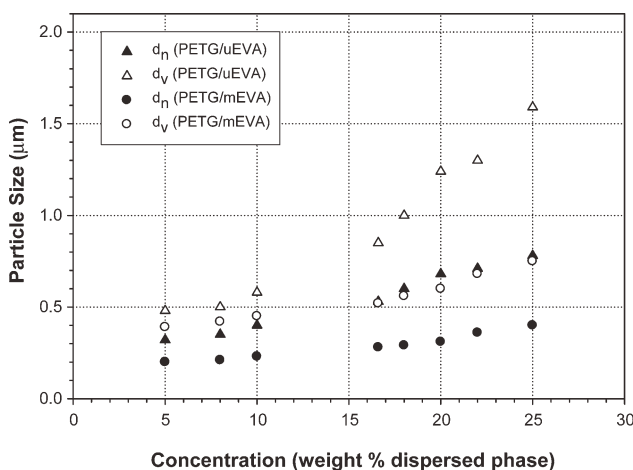


Figure 2. Dispersed particle size (μm) versus concentration of uEVA or mEVA in PETG matrix.

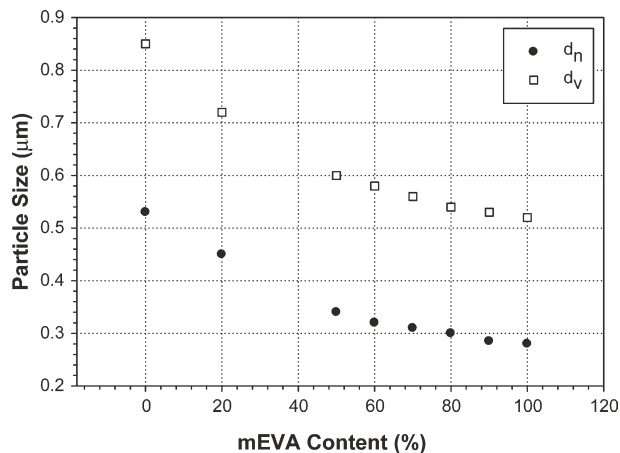


Figure 3. Dispersed particle size (μm) as a function of mEVA content in the dispersed phase for of PETG/EVA/mEVA blends with fixed dispersed phase content 20 phr.

prepared by changing the composition of uEVA and mEVA whereas total EVA content was fixed at 20 phr. The ductile–brittle transition occurred at 78–80 wt % of the mEVA content in Figure 5. A significant decrease of the impact strength was found at specific mEVA content as the compatibility increases.

Toughening Mechanism

Figure 6 showed the SEM micrograph of the impact-fractured surface of PETG/mEVA blend under the low magnification (×40). The fracture surface shows a fast crack growth for an entire specimen except for near the notched area (a).^{25,26}

The SEM micrograph with a high magnification of (a) and (b) in Figure 6 was presented in Figure 7. The cavitation and shear deformation were observed in (a-1) whereas shear deformation was not found in (a-2). In addition, no cavitation and shear deformation was found in the area behind (a-2) area in Figure 6, and the clear division between PETG matrix and dispersed EVA phase with a fast crack growth to the end of specimen was observed. It is believed that the crack growth of the specimen was fast, and the cavitation of dispersed mEVA was limited at

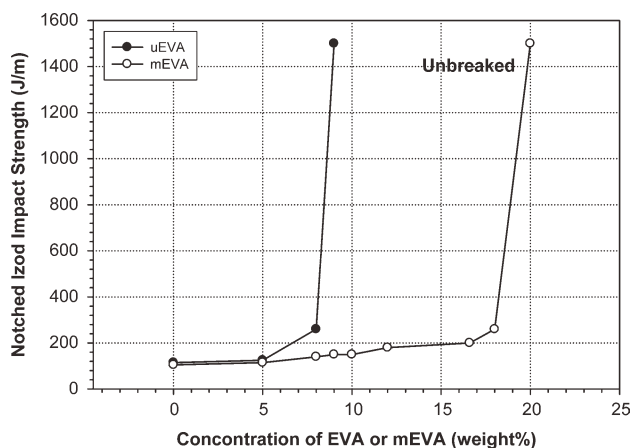


Figure 4. Impact strength versus concentration of uEVA or mEVA in PETG matrix.

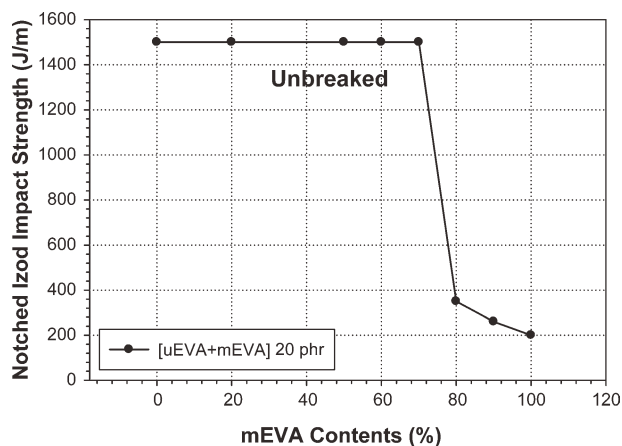


Figure 5. Impact strength as a function of mEVA content in the dispersed phase for PETG/uEVA/mEVA blends with a fixed dispersed phase content of 20 phr.

near notched part, and the shear deformation was found in smaller area of notched part of PETG/mEVA (20 phr) blend. It can be seen that although the cavitation and shear deformation were observed, the blend showed brittleness because both behaviors occurred at very small area.

Figure 8 presents the SEM micrograph of fractured surface of PETG/uEVA blend. The specimen was not completely broken showing a strong toughness. No trace of a fast crack growth was

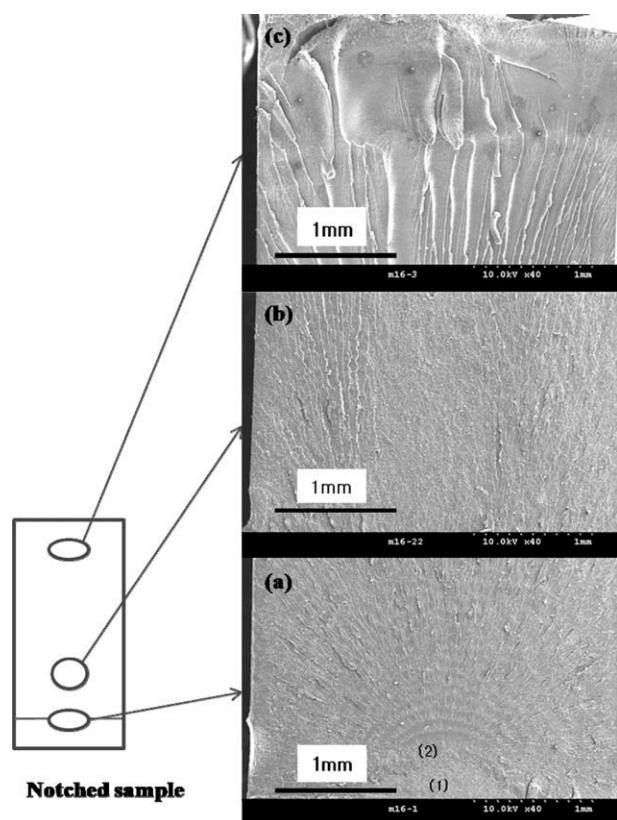


Figure 6. SEM micrographs of impact-fractured surface of PETG/mEVA (20 phr) blend under the low magnifications.

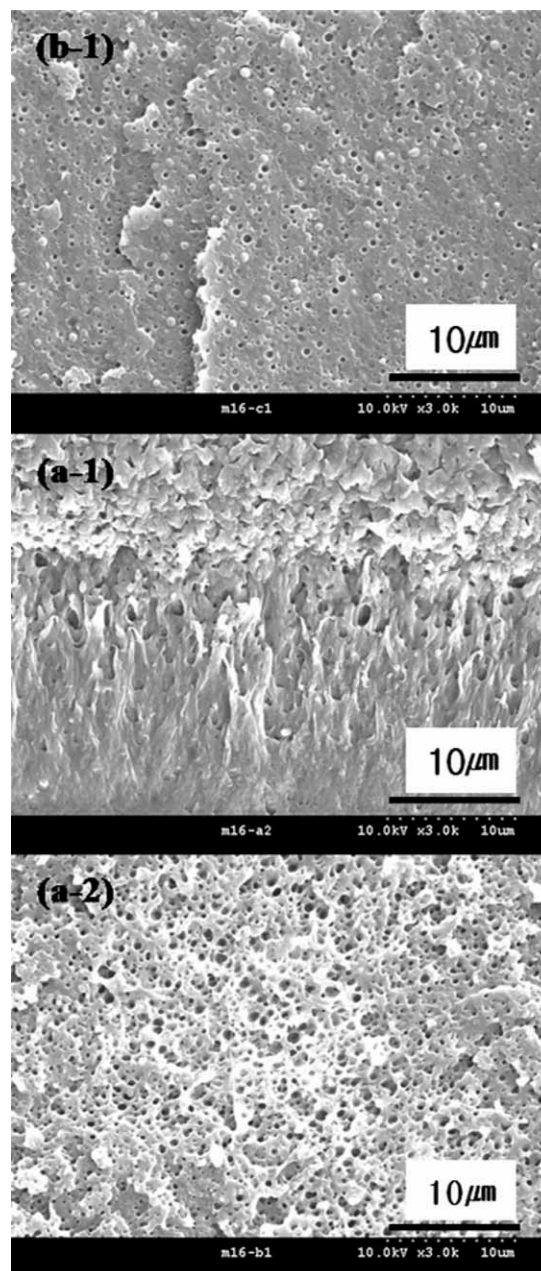


Figure 7. SEM micrographs of impact-fractured surface of PETG/mEVA (20 phr) blend under the high magnifications.

observed at the low magnification in (a) and (b), but the shear deformation of the PETG matrix was found in (a-1) and (b-1) at the high magnification.

Through the SEM observation, the cavitation of rubber particle and shear deformation of the PETG matrix was observed, and the shear deformation was found at the broad range for the blend with a strong toughness. It can be concluded that the toughening mechanism of the PETG/EVA blend is the shear deformation induced by the cavitation. In addition, it was confirmed that the cavitation can be a necessary condition for shear deformation, but cannot be a sufficient condition.

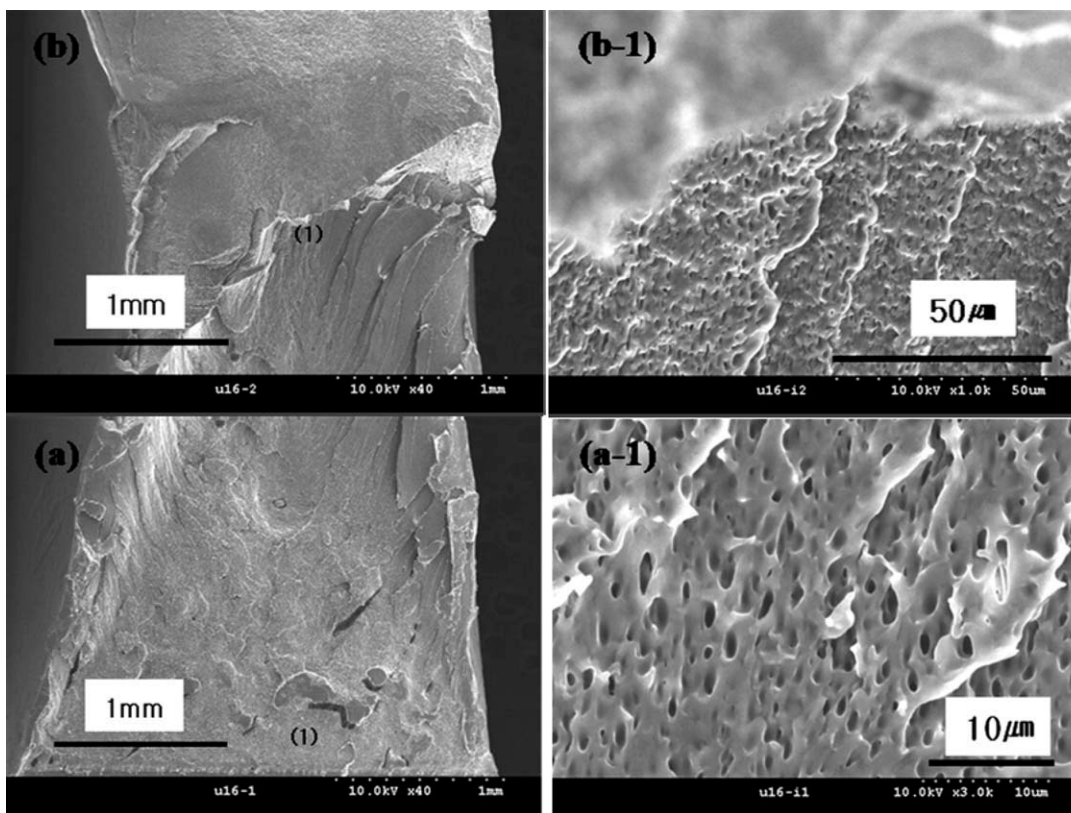


Figure 8. SEM micrographs of impact-fractured surface of PETG/mEVA (20 phr) blend under the low and high magnifications.

The Morphological Effect on the Brittle–Ductile Transition

The cause of brittle–ductile transition at various compositions of mEVA and uEVA was investigated. As mentioned in the introduction section, the cavitation of rubber particle and the shear deformation was considerably affected by morphology. The inter-particle distance was obtained from the particle diameter and volume fraction, and the relationship with the impact strength was investigated. The volume fraction of dispersed particle was obtained from the following equation.

$$\Phi_d = \rho_m \omega_d / \{(\rho_m - \rho_d) \omega_d + \rho_d\}$$

where ρ_m and ρ_d are the density of matrix and dispersed phase, respectively, and ω_d is volume fraction of dispersed phase.

Figure 9 showed the impact strength with inter-particle distance of various compositions of PETG/mEVA and PETG/uEVA blend. Both blends showed a good toughness in certain periods, and the transition occurred at 0.08–0.1 μm of inter-particle distance for mEVA whereas the transition of uEVA was found at 0.24–0.26 μm .

The effect of inter-particle distance on the impact strength of the PETG/uEVA/mEVA blend with changing the composition of mEVA and uEVA content while total EVA content was fixed at 20 phr was given in Figure 10. The brittle–ductile transition was found at about 0.11 μm , and the blend showed toughness beyond this point. This is the opposite result from Figure 9. The blend having smaller inter-particle distance than that of the

transition point showed toughness in Figure 9, and this may be due to the effect of rubber content rather than inter-particle distance. Therefore, the result from Figure 10 in PETG/EVA blend system was not consistent with the results of the Wu’s study with Nylon/rubber system showing that smaller inter-particle distance had effect on improving the toughness.

The relationship of number average particle diameter (d_n) and volume average particle diameter (d_v) with the impact strength were presented in Figures 11 and 12, respectively. The

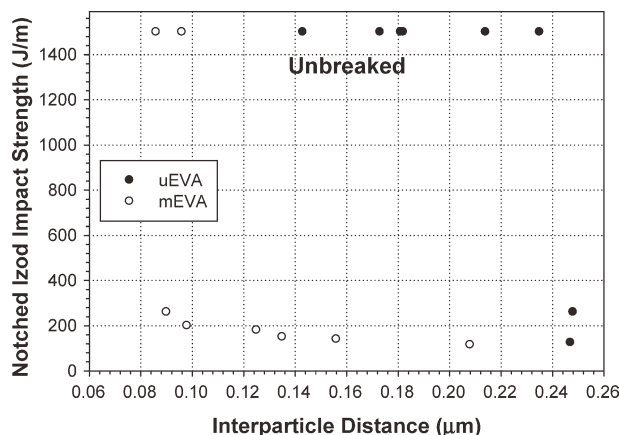


Figure 9. Impact strength versus inter-particle distance (τ) of dispersed phase EVA or mEVA in PETG matrix.

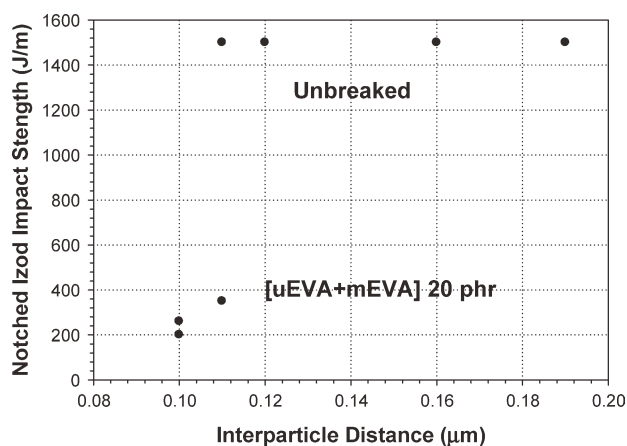


Figure 10. Impact strength as a function of inter-particle distance in the dispersed phase for PETG/EVA/mEVA blends with a fixed dispersed phase content of 20 phr.

brittle–ductile transition was found at d_n : 0.37 μm and d_v : 0.54 μm for dispersed mEVA whereas d_n : 0.30 μm and d_v : 0.58 μm was transition point for uEVA, respectively. The toughness appeared at beyond those critical particle diameters, and the transition phenomenon was significantly dependent on dispersed particle diameter regardless of modification of EVA.

Same behavior was found on the test with various compositions of mEVA and uEVA of the PETG/uEVA/mEVA blend whereas the total dispersed EVA content was fixed at 20 phr. The transition occurred at the critical particle diameter (d_n : 0.30 μm and d_v : 0.55 μm) showing toughness beyond this point (Figure 13). Therefore, it can be concluded that the brittle–ductile transition occurred at critical particle diameter in PETG/EVA blend system, and the toughness appeared above this minimum critical particle diameter.

The MAH as reactive compatibilizer decreased the particle diameter of dispersed EVA in the PETG/EVA blend, so this decrease of particle diameter induced by the increase of compatibility results in ductile–brittle transition on the blend, and this

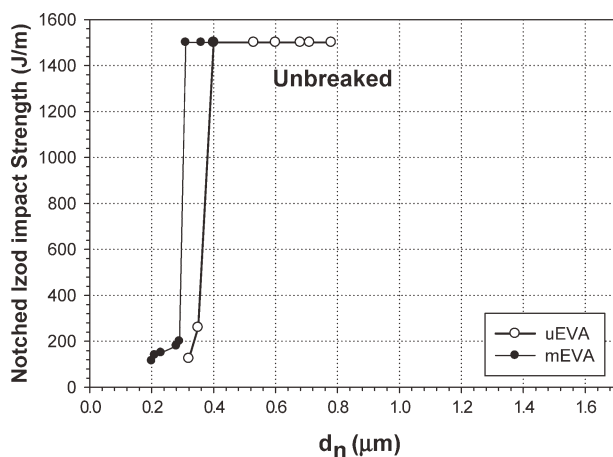


Figure 11. Impact strength versus dispersed number average particle diameter of EVA or mEVA in PETG.

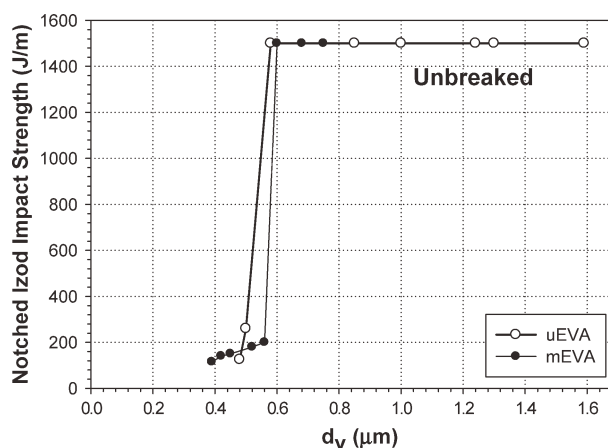


Figure 12. Impact strength versus dispersed volume average particle diameter of EVA or mEVA in PETG.

is consistent with the fact that the rubber particle should have bigger particle diameter than the minimum critical diameter to have cavitation by Dompas and Bucknall.

CONCLUSIONS

The cavitation and shear deformation in matrix phase of the rubber particle was investigated from the morphological observation. It was confirmed that the shear deformation induced by the cavitation was a toughening mechanism for PETG/EVA blend, and the cavitation could be a necessary condition for shear deformation, and could not be a sufficient condition. The brittle–ductile transition was found at about d_n : 0.37 μm and d_v : 0.55 μm of particle diameter, a critical particle diameter, regardless of EVA content, the blend showed ductility beyond the critical particle diameter. Therefore, the brittle–ductile transition in this PETG/EVA blend system occurred at beyond.

The amount of mEVA, required to induce brittle–ductile transition of the blend was about 20% and those of EVA was about 10% concentrations. This means that to increase toughness of PETG/EVA blend, dispersed phase has to have over critical

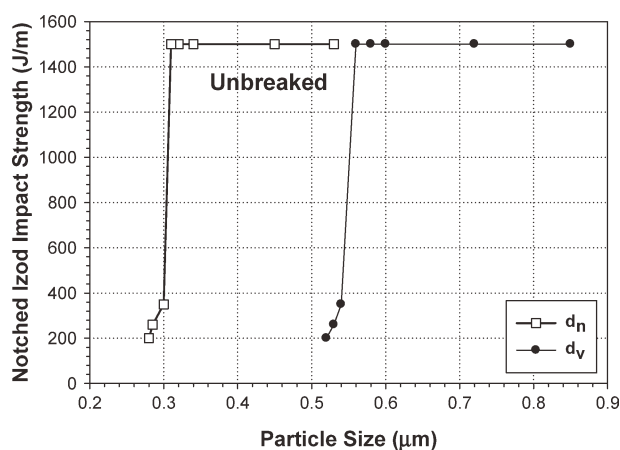


Figure 13. Impact strength as a function of particle diameter in the dispersed phase for PETG/EVA/mEVA blends with a fixed dispersed phase content of 20 phr.

particle size, and to reach this particle size, larger amount of mEVA was needed in the case of mEVA. Contrary to Wu's researches on Nylon/rubber system, the inter-particle distance of mEVA particle at brittle–ductile transition was not coincident with that of uEVA(unmodified EVA).

To investigate the effects of particle size on the toughness of blend system, while eliminating the influence of the content of dispersed phase, the amount of dispersed phase was fixed at 20 phr and dispersed particle size was varied by adjusting the mixing ratio of EVA and mEVA. As mentioned earlier, the mixing ratio of mEVA increased, the particle size and inter-particle distance decreased.

When over 80% of mEVA was used, the Izod sample was brittle, and the brittle–ductile transition occurred between 78% and 80% of mEVA. The critical particle size, at which brittle–ductile transition was occurred, was 0.3 μm of number average diameter and 0.55 μm of volume average diameter. Explained by Buknall and Dompas, the presence of the minimum inter-particle distance, over which the blend became ductile, was confirmed.

With the observation of fractured surface it was thought that the toughening of PETG/EVA system resulted from shear deformation, induced by cavitation of dispersed EVA particles.

REFERENCES

- Paul, D. R.; Bucknall, C. B. *Polymer Blends*; John Wiley & Sons: New York, **1999**.
- Raymond, A.; Pearson, I.; Sue, H. J.; Yee, A. F. *Toughening of Plastics*; American Chemical Society: Washington, DC, **2000**.
- Dagli, G.; Argon, A. S.; Cohen, R. E. *Polymer* **1995**, *36*, 2173.
- Muratoglu, O. K.; Argon, A. S.; Cohen, R. E. *Polymer* **1995**, *36*, 921.
- Margolina, A.; Wu, S. *Polymer* **1988**, *29*, 2170.
- Bagheri, R.; Reardon, R. A. *Polymer* **1996**, *37*, 4529.
- Pearson, R. A.; Yee, A. F. *J. Mater. Sci.* **1991**, *26*, 3828.
- Cho, K.; Yang, J.; Pank, C. E. *Polymer* **1997**, *38*, 5161.
- Ayre, D. S.; Bucknall, C. B. *Polymer* **1998**, *39*, 4785.
- Lazzeri, A.; Bucknall, C. B. *Polymer* **1995**, *36*, 2895.
- Yu, Z. Z.; Lei, M.; Ou, Y.; Yang, G. *Polymer* **2002**, *43*, 6993.
- Yu, Z. Z.; Lei, M.; Ou, Y.; Yang, G. *J. Appl. Polym. Sci.* **2003**, *89*, 797.
- Jiang, W.; Tjong, S. C.; Li, R. K. Y. *Polymer* **2000**, *41*, 3479.
- Jiang, W.; Yuan, Q.; An, L.; Jiang, B. *Polymer* **2002**, *43*, 1555.
- Hale, W.; Lee, J. H.; Keskkula, H.; Paul, D. R. *Polymer* **1999**, *40*, 3621.
- Lacroix, C.; Bousmina, M.; Carreau, P. J.; Favis, B. D. *Polymer* **1996**, *37*, 2939.
- Graebing, D.; Muller, R.; Palierne, J. F. *Macromolecules* **1993**, *26*, 320.
- Iza, M.; Bousmina, M.; Jerome, R. *Rheol. Acta* **2001**, *40*, 10.
- Wu, S. *Polymer* **1985**, *26*, 1855.
- Dompas, D.; Groeninckx, G. *Polymer* **1994**, *35*, 4743.
- Dompas, D.; Groeninckx, G.; Isogawa, M.; Hasegawa, T.; Kadokura, M. *Polymer* **1994**, *35*, 4750.
- Dompas, D.; Groeninckx, G.; Isogawa, M.; Hasegawa, T.; Kadokura, M. *Polymer* **1994**, *35*, 4760.
- Lazzeri, A.; Bucknall, C. B. *Polymer* **1995**, *36*, 2895.
- Hwang, S. W.; Ryu, H. C.; Kim, S. W.; Park, H. Y.; Seo, K. H. *J. Appl. Polym. Sci.* **2012**. DOI 10.1002/app.36592.
- Newman, S. B.; Wolock, I. J. *Appl. Phys.* **1958**, *29*, 49.
- Wolock, I.; Kies, J. A.; Newman, S. B. *Fracture*; New York: Wiley, **1959**.